Diffusive light transport in semitransparent media

Lorenzo Pattelli,[1] Giacomo Mazzamuto,[1,2] Diederik S. Wiersma,[1,3] and Costanza Toninelli[1,2,4,*]
[1]*European Laboratory for Non-linear Spectroscopy (LENS), 50019 Sesto Fiorentino, Florence, Italy*
[2]*Istituto Nazionale di Ottica (CNR-INO), Via Carrara 1, 50019 Sesto Fiorentino, Florence, Italy*
[3]*Department of Physics, Università di Firenze, 50019 Sesto Fiorentino, Florence, Italy*
[4]*QSTAR, Largo Enrico Fermi 2, 50125 Florence, Italy*
(Received 22 September 2015; published 24 October 2016)

It is common knowledge that diffusion theory cannot describe light propagation in semitransparent media, i.e., media with a low optical thickness. However, even in an optically thin slab, late-time transport will be eventually determined by a multiple scattering process whose characteristics are still largely unexplored. We numerically demonstrate that, even for an optical thickness as low as 1, after a short transient, propagation along the slab plane becomes diffusive. Nonetheless, we show that such a diffusion process is governed by modified statistical distributions which result from a highly nontrivial interplay with boundary conditions.

DOI: 10.1103/PhysRevA.94.043846

I. INTRODUCTION

The physics of light transport in scattering materials represents an intensive research field both for its fundamental interest and for its applications [1]. In this ubiquitous class of media, light coherence and polarization typically do not play a significant role and the transport problem can be modeled as a random walk of energy packets determined by microscopic parameters such as the scattering mean free path l_s, the absorption length l_a, and the scattering anisotropy g, defined as the average cosine of the scattering angle. The problem simplifies significantly with the onset of the multiple scattering regime which typically characterizes thick and turbid samples. In this case, after a short transient, transport becomes diffusive and is characterized by an isotropic transport mean free path $l_t = l_s/(1-g)$, allowing a description in terms of the simple, analytic diffusive approximation (DA). Focusing on late, multiply scattered light, the relation $D_{DA} = v l_t/3$ links the diffusion coefficient D_{DA} to the microscopic transport mean free path l_t through the energy velocity v inside the sample [2,3]. This connection proves crucial in many different fields, making it possible to probe the microscopic structural properties of an unknown medium by measuring the macroscopic rate at which light diffuses through it. In practice, however, the validity of the diffusive approximation is limited to samples with a thickness L_0 at least 1 order of magnitude bigger than l_t [4]. When this is not the case, the sample appears semitransparent and the diffusion approximation breaks down in the sense that light transport will be dominated by unscattered (ballistic) light, or light undergoing too few scattering events. Despite the large relevance of optically thin membranes in fundamental research [5–8] and applications [9–13], this class of samples remains to date less studied given the need for nonapproximated numerical techniques.

In this work we reveal and elucidate the peculiar features of light transport in optically thin slabs. By performing extremely large Monte Carlo simulations we are able to investigate the late-time propagation of light deeply in the multiple scattering regime, which results in a fully developed diffusive transport along the plane of the slab even at very low turbidity. Recent numerical and experimental evidence [14–16] suggests that studying transport along transverse directions provides observables that are more robust against experimental uncertainties and easier to interpret within the diffusion approximation, as opposed to other observables such as the decay time τ of the spatially integrated transmission. Nevertheless, the vast literature available for the slab geometry typically focuses on axial rather than transverse transport [4–6,8,17–20], which therefore remains still largely unexplored. Here we show how investigating transverse transport provides fundamental insight to our understanding of light propagation in scattering media, and we illustrate how boundary conditions *modify the very statistical distributions underlying the radiative transport process*.

II. TRANSVERSE TRANSPORT IN A SLAB GEOMETRY

According to diffusion theory, the instantaneous intensity profile transmitted through a turbid slab is Gaussian $I(\rho,t) \propto \exp[-\rho^2/w^2(t)]$ with a mean square width (MSW) growing linearly with time as $w^2(t) = 4D_{DA}t$ [2]. Such a width represents the variance of the profile, which is independent of the instantaneous integrated intensity and is more generally defined for an arbitrary distribution $I(\rho,t)$ as

$$w^2(t) = \frac{\int_0^\infty \rho^2 I(\rho,t) d^2\rho}{\int_0^\infty I(\rho,t) d^2\rho}, \tag{1}$$

with ρ representing a two-dimensional vector in the transmission plane. Remarkably, the mean square width w^2 is independent of absorption (which cancels out exactly at any time [21]) and, according to the simple diffusive model, it is also independent of both the slab thickness and its refractive index contrast with the environment. The mean square width therefore represents a largely appealing quantity to be investigated, allowing one to retrieve the microscopic transport mean free path l_t, even if the thickness and the refractive index contrasts are not known precisely [15], and without being affected by the typical cross-talk artifacts due to absorption [14,16].

*toninelli@lens.unifi.it

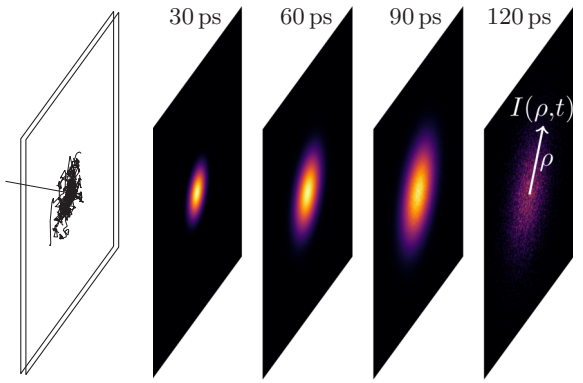

FIG. 1. Sketch of the configuration used for Monte Carlo simulations. An infinite slab is illuminated by a pencil beam pulse $\delta(t)\delta(r)$ of energy packets performing a random walk inside the scattering material. A few representative trajectories and normalized transmitted intensities are shown in the case of an optically thin, index-matched slab ($n_{\rm in} = n_{\rm out} = 1$) with thickness $L_0 = l_{\rm s} = 1$ mm and scattering anisotropy $g = 0$.

Taking advantage of these properties, we make use of the MSW growth to study transverse diffusive transport in optically thin slabs. This makes our analysis exactly independent from absorption, which can be therefore ignored in the simulations. In our Monte Carlo simulations, a pencil beam pulse $\delta(t)\delta(r)$ of energy packets impinges on a thin slab of scattering material (see Fig. 1). The energy packets propagate performing a random walk according to an exponential step length distribution and a Heyney-Greenstein phase function. For the sake of convenience, given that Fresnel reflection coefficients depend solely on the ratio n, we kept $n_{\rm in} = 1$ constant in order to have a consistent time scale for each simulation. Results for any arbitrary $n_{\rm in}$ and $n_{\rm out} = n_{\rm in}/n$ pair can be retrieved exactly with a simple rescaling operation. For each transmitted particle, we consider the distance ρ between its exit point and the optical axis. The integrals in Eq. (1) are then evaluated as finite summations over the particles transmitted within a certain time window. We considered scattering slabs with an optical thickness (OT) of $L_0/l_{\rm t} = 1$, with $L_0 = l_{\rm t} = 1$ mm. We observe that, after a short transient, the mean square width grows linearly in time as shown in Fig. 2(a), which is a clear hallmark of diffusive propagation. Excluding a time window of 4τ is always sufficient to reach the diffusing regime for all values of n and g, at OT $= 1$. Expressing time axes in units of the decay time τ of the corresponding spatially integrated transmission allows one to get an estimate of the fraction of energy packets involved at each point. For example, the fraction of packets reaching this diffusive regime is of the order of percent [$\sim \exp(-4)$], which is largely significant experimentally given that common time-resolved techniques span up to 8 decades of dynamic range [22]. For each simulated configuration, an observed diffusion coefficient D can be extracted from a linear fit of the $w^2(t > 4\tau)$ curves, as $1/4$ of the asymptotic slope.

To our knowledge, the validity range of the simple linear prediction $w^2(t) = 4D_{\rm DA}t = 4vl_{\rm t}t/3$ cast by diffusion theory has not been tested to date. Obviously, at an OT as low as 1, high deviations are observed [Fig. 2(b)]. Remarkably, the

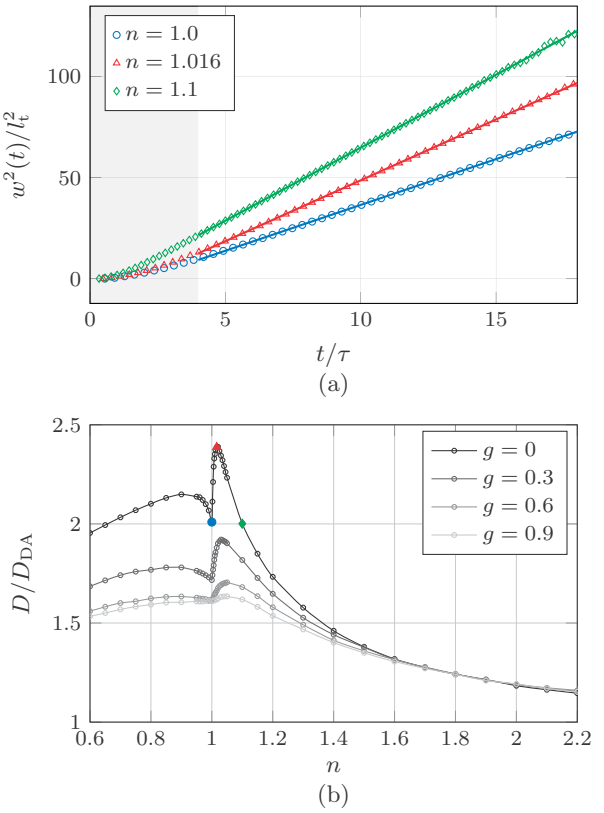

FIG. 2. (a) MSW expansion for three slab configurations with $l_{\rm t} = L_0$, $g = 0$, and different refractive index contrasts, showing a perfectly linear growth after a short transient (shaded). (b) Dependence on the refractive index contrast n and scattering anisotropy g of the diffusion coefficient D as inferred from a linear fit of the mean square width $w^2(t > 4\tau)$ for different samples with OT $= 1$. Solid points represent the values retrieved from the linear fits shown in panel (a).

largest deviations are found in the proximity of $n = 1$, which is usually quoted as a safer configuration for the diffusion approximation [20]. It is also worth noting that the MSW slope of the simulated data is always greater than the value expected from diffusion theory, i.e., the diffusion coefficient appears to be enhanced. A first, qualitative explanation for this enhancement can be attempted based on the d-dimensional modeling of diffusion as a random walk process, which, given a step length distribution $P(l)$ with finite moments $\langle l\rangle$ and $\langle l^2\rangle$, predicts a mean square d-dimensional displacement growing as $2d\,Dt$ with

$$D = \frac{1}{2d} v \frac{\langle l^2\rangle}{\langle l\rangle} = \frac{1}{d} v l_{\rm t}, \tag{2}$$

where the last equality holds for an exponential step-length distribution with average step length $l_{\rm t}$ [23]. As the optical thickness of the simulated slab decreases, transport occurs in an increasingly planar geometry. Hence, as suggested by Eq. (2), the effective diffusion coefficient D as inferred from the MSW slope might be up to $3/2$ times higher than its bulk nominal value. The perceived spatial dimensionality is also affected by the refractive index contrast. Near $n = 1$, any energy packet leaving the sample at long times will have performed an almost

planar trajectory, akin to a purely two-dimensional walk. On the contrary, strong boundary reflections allow trajectories to fold back into the sample, which is therefore perceived more as a three-dimensional environment [which also explains why the diffusive approximation recovers gradually for high values of the refractive index contrast, see Fig. 2(b)]. A closer look at the data, however, shows that diffusion exhibits a local *minimum* at $n = 1$, rather than a maximum, with the D/D_{DA} ratio exhibiting a sharp modulation across the index-matching condition. Around $n = 1$, diffusion appears to be asymmetrically enhanced, reaching an absolute maximum around $n = 1.016$ for $g = 0$.

III. EFFECTIVE RANDOM WALK STATISTICS

In order to explain the origin of such deviations, we focus on three significant configurations [highlighted as solid symbols in Fig. 2(b)] representing key points of the observed peak for $g = 0$, i.e., $n = 1$, 1.016, and 1.1. These three particular configurations were further investigated to collect detailed statistics at long times, with 10^{14}, 0.5×10^{14}, and 10^{13} energy packets each. Dealing with simulations of this magnitude required the development of a dedicated implementation of the standard Monte Carlo method, in order to accurately generate and represent the large number of random variates involved in the simulations [15].

As suggested by Eq. (2), the most straightforward insight on the diffusion coefficient D is obtained by directly looking at the distribution of the step lengths performed during the random walk. In principle, each trajectory is generated according to the same exponential step-length distribution $P(l) = l_{\mathrm{s}}^{-1} \exp(-l/l_{\mathrm{s}})$. However, we find that the finite thickness of the slab configuration induces a positive correlation between a long permanence inside the sample and a higher probability of drawing longer step lengths. Figure 3 shows the histograms of the step lengths and scattering angles between two consecutive scattering events for those energy packets that were transmitted at $t = 90$ ps (corresponding to a path length of $\approx 27 L_0$) compared with their nominal distributions implemented in the Monte Carlo algorithm (dashed lines). The step-length distributions [Fig. 3(a)] exhibit enhanced tails for all three simulated refractive index contrasts, consistently with the observed enhancement of the diffusion rate [cf. Eq. (2)]. In this thin slab geometry, the nominal step-length distribution provided by the pseudorandom number generator is sampled unevenly in such a way that all its moments are significantly modified: despite the fact that a long step in a very thin sample will generally cause the packet to exit the slab, those few packets that happen to remain inside will be able to reach long surviving times without undergoing many scattering events. In the case of refractive index contrasts close to 1, the distribution of the step lengths features a selective enhancement of the longer values, which is slightly more marked for $n = 1.016$. This is due to the fact that, even for such a small refractive index contrast, total internal reflection is already significant ($\theta_{\mathrm{c}} = 79.8^{\circ}$). If internal reflections are absent, extremely narrow angular conditions must hold in order for the packet not to exit the slab. Conversely, even a tiny contrast allows one to largely relax such a condition, introducing a significant increase in the survival probability of

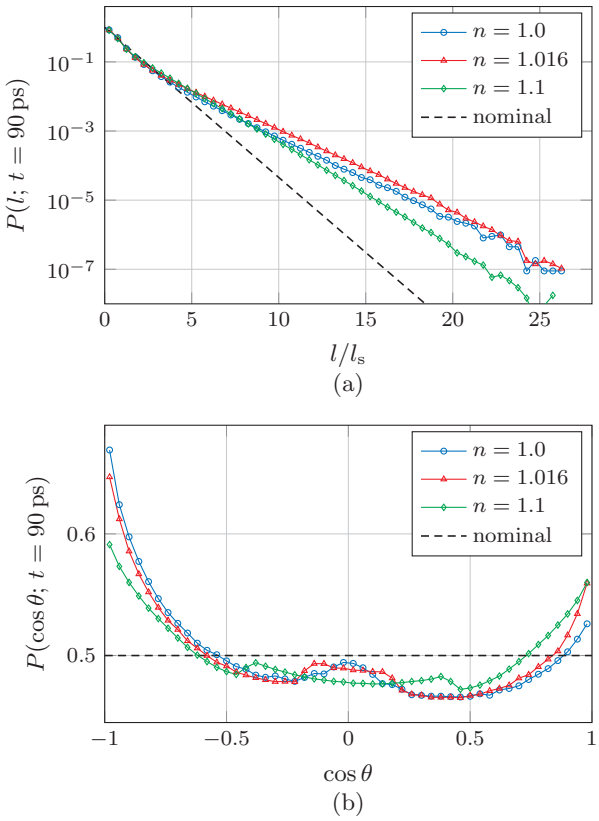

FIG. 3. Late-time modification of the step-length and scattering-angle distributions for an optically thin slab with OT $= 1$, $g = 0$, and $n = 1$, 1.016, and 1.1. Panel (a) shows the probability distribution of step lengths between consecutive scattering events performed by those energy packets that are transmitted at $t = 90$ ps. The retrieved distributions exhibit heavier tails than the nominal one (dashed line). Scattering angles become unevenly sampled at late times as well, as shown in panel (b).

a long-stepping energy packet while only marginally affecting others. In short, there is a positive correlation between long steps and shallow incidence angles, whose effects become apparent when such angles are the only ones undergoing total internal reflection [which also explains why the enhancement shown in Fig. 2(a) is asymmetric around $n = 1$]. On the other hand, with increasing contrast, more energy packets will be held inside the slab irrespective of their incidence angle (and hence of the length of their step), thus weakening the observed enhancement in the MSW growth rate.

Interestingly, the sampling of the angular variables is also modified at late times, as shown in Fig. 3(b) for the same set of simulations. While tracing each random trajectory, the cosines of the scattering (polar) angles θ are generated uniformly in $[-1, 1]$ through the pseudorandom number generator. On the contrary, the observed asymptotic $\cos\theta$ distribution exhibits two peaks for backwards and forward scattering. This can be intuitively understood by considering the fact that typical steps in a very long trajectory will be mostly aligned with the slab plane. As such, scattering angles close to $\theta = 0^{\circ}$ or 180° guarantee that the trajectory will continue within the slab irrespective of what azimuthal angle is drawn. Actually, since a typical step will not be in general perfectly parallel to

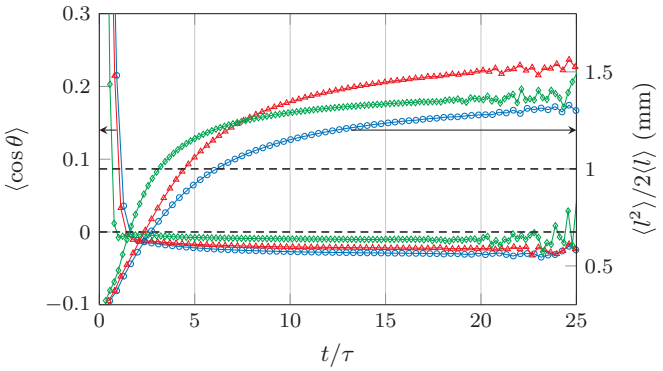

FIG. 4. Time evolution of the ratio $\langle l^2 \rangle / 2\langle l \rangle$ appearing in Eq. (2) and of $\langle \cos\theta \rangle$, as obtained by the simulations. Each point is obtained considering only the energy packets transmitted within the corresponding time bin. Dashed lines represent the nominal values for the two distributions.

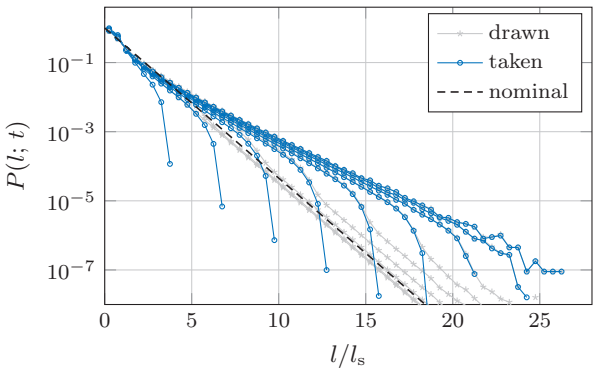

FIG. 5. Time evolution of the step length distribution for $n = 1$ for energy packets transmitted at $t = 10$, 20, 30, 40, 50, 60, 70, 80, and 90 ps. The gray curves and the blue curves show, respectively, the histogram of the step lengths drawn through the pseudorandom number generator and of the steps taken inside the sample. The two only differ for the last step of each trajectory.

the interfaces, a scattering angle of $\theta \approx 180^\circ$ should provide higher chances of staying inside the sample, hence its higher probability. This results in a $\cos\theta$ distribution with a slightly negative average value (Fig. 4, left axis), which also plays a role in determining the effective diffusion properties exhibited by the sample.

With reference to Eq. (2), we plot the quantity $\langle l^2 \rangle / 2\langle l \rangle$ in Fig. 4 (right axis), along with its nominal value of 1 (dashed line). At long times, each curve seems to saturate to an asymptotic value, suggesting the existence of a well-defined effective diffusion coefficient. The random-walk-based picture of diffusion as expressed by Eq. (2) is qualitatively supported by the fact that also this figure of merit is enhanced for $n = 1.016$ (red curve), in accordance with Fig. 2(a). In principle, the overall diffusion process will be influenced by both the modified step length and angular statistics, which in the investigated configurations appear to have opposite effects, as also shown in Fig. 4. While the latter would indeed tend to slightly slow down diffusion, the predominant effect is coming from the step lengths being substantially increased, leading to the observed enhanced in-plane diffusion especially for $n = 1.016$. Notably, different configurations might lead to a different balance between these two effects, which also appear to saturate to their respective asymptotic values on slightly different time scales, further illustrating the need for additional investigations even for the simple model of a homogeneous and isotropic single slab.

The asymptotic nature of the effective diffusion coefficient in a thin slab is further highlighted in Fig. 5, where the time evolution of the step-length distribution is shown for $n = 1$ (the $n = 1.016$ and 1.1 cases are analogous). The time-resolved distributions seem to converge towards a single asymptotic envelope distribution with a well-defined asymptotic decay rate which seems to be uniquely determined by the properties of the sample. It is interesting to compare the histogram of the actual steps performed inside the sample (blue curves) with the histogram of the ones drawn through the pseudorandom number generator (gray curves). The two differ only for the last step, whose length is respectively considered either partially (up to the interface) or totally. At late times the two sets of curves become indistinguishable since, as expected, the contribution of the last step to the whole trajectory becomes eventually statistically negligible.

As a result of the transport statistics being directly altered by the sample configuration, an optically thin sample generally appears to be less scattering than it actually is. In other words, once the diffusive regime is reached, energy packets propagate as if scatterers were further apart than they actually are, i.e., with an *effective* transport mean free path greater than the one *intrinsic* to the material. Albeit smaller, similar discrepancies have been reported even in samples with an optical thickness as high as 8 [16], suggesting that modifications of transport statistics could be still appreciable in more turbid media.

IV. DECAY TIME OF INTEGRATED TRANSMISSION

Before drawing conclusions, it is interesting to note that a qualitatively similar behavior to what we described for the mean square width [Figure 2(b)] is also found in the relative deviations of decay times from the diffusive prediction [Fig. 6(a)] and is therefore not strictly limited to the propagation of light along the slab plane. It is worth discussing this point separately, especially given that decay time measurements of integrated transmittance have long been experimentally accessible and exploited to estimate the diffusion coefficient via the expression (for a nonabsorbing medium)

$$\tau_{\mathrm{DA}} = \frac{L_{\mathrm{eff}}^2}{\pi^2 D_{\mathrm{DA}}}, \tag{3}$$

where $L_{\mathrm{eff}} = L_0 + 2z_{\mathrm{e}}$ is the effective thickness of the medium and z_{e} represents the extrapolated length for a given refractive index contrast.

A similar dependence on n with respect to the previous case can be appreciated in Fig. 6(a), where we plot the ratio between the decay time τ as fitted from the Monte Carlo simulations and the decay time τ_{DA} as computed from Eq. (3). As opposed to the previous case, however, the τ/τ_{DA} ratio can evidently take values both above and below 1, depending subtly on the scattering anisotropy and the refractive

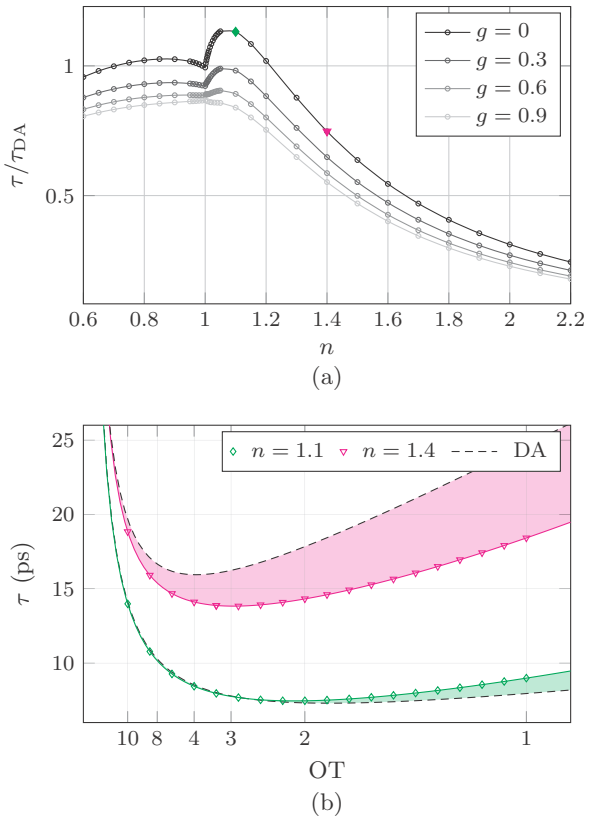

FIG. 6. (a) Dependence on the refractive index contrast n and scattering anisotropy g of the decay time τ as inferred from a single-exponential fit of the spatially integrated transmitted intensity for $\mathrm{OT} = 1$. Especially for lower g factors, the ratio can clearly go above 1 for certain values of the refractive index contrast. The dependence of τ on OT for values highlighted as filled symbols is shown in panel (b). Dashed lines represent the DA prediction; solid lines serve as guides to the eye.

index contrast of the sample. This observation might explain why retrieving the diffusion coefficient from a decay time measurement using Eq. (3) is sometimes regarded as a poor estimation, since this can lead both to over- or underestimated values [4]. This is further illustrated in Fig. 6(b) for a couple of representative cases exhibiting opposite deviations that can persist even at higher optical thicknesses. This behavior is particularly interesting considering that, to date, experimental data and theoretical predictions are inconsistent. While the former bring generally evidence suggesting that retrieving D_{DA} through a decay time measurement would lead to a decreasing diffusion coefficient with decreasing thickness [24,25], the latter have so far mainly provided arguments in favor of the opposite behavior [4,19,26,27]. In this respect, our simulations show that there is a region in the parameter space where the τ/τ_{DA} ratio exceeds 1, which can lead to the experimentally observed decreasing diffusion coefficient with decreasing thickness. The analysis on the decay times confirms the importance of an accurate and precise modeling of the index contrast, which we think has been often overlooked, for example, by considering a symmetric averaged contrast to model asymmetric experimental configurations [4,19,26].

V. CONCLUSIONS

To conclude, we have studied the diffusive transport regime in optically thin samples, which develops at late times in the slab plane and shows peculiar features especially for small refractive index contrasts. Due to the asymptotic nature of this transport regime, our results apply indifferently to transmission and reflection collection geometries.

Our investigation revealed a subtle interplay occurring between the actual thickness of the slab, the refractive index contrast, and the scattering anisotropy, determining a transport regime that is diffusive on long time scales but which cannot be described in terms of the simple diffusive approximation. A different and asymptotic diffusion coefficient naturally emerges from the overall optical and geometric boundary conditions of the sample and is univocally determined by them through yet unknown relations. In this respect, our findings recall a recently published work where it is analogously demonstrated that the link between microscopic (i.e., the scattering coefficient) and macroscopic (i.e., the diffusion coefficient) transport parameters remains unknown for diffusive anisotropic media [28]. Analogously, our results show that this link should be further investigated even in the isotropic case, especially for weakly scattering media. In particular, concerning microscopic optical properties such as g or l_{t}, it seems appropriate to introduce a distinction between an intrinsic and an effective counterpart, where the former is the one that we are typically interested in retrieving while the latter might have a very different value and nature (e.g., tensorial instead of scalar) depending on incidental geometric conditions. It must be noted that the lack of an analytical description of the deviations that we unveiled does not hinder their practical utility. On the contrary, this effect provides a unique opportunity to directly infer the unknown intrinsic optical parameters through, e.g., parametrization or a look-up table approach [15].

The enhanced diffusive regime that we described should not be confused with faster-than-diffusion transport phenomena [29,30], which describe very different systems where diffusion does not apply. Analogously, it is worth stressing that the effect that we unveiled is fundamentally different from apparently similar boundary effects described in the literature [31,32], which can be usually taken into account through some refined extrapolated boundary conditions. This cannot be the case here, since extrapolated boundary conditions correct significantly quantities such as the total transmittance which, conversely, would be hardly affected by asymptotic modifications of the effective diffusion coefficient. Indeed, because of the asymptotic nature of these effects, only a small fraction of the incoming light is actually subject to this effective transport mean free path when studying thin samples. Yet, the effect is largely accessible experimentally [22] and similar deviations have in fact already been observed directly [16]. Moreover, other applications can be envisioned where multiple scattering in thin layers, even if limited to a very small fraction of incident light, could play a significant role (e.g., random lasers). In this respect, we demonstrated how the interplay between transport properties and the environment geometry can give rise to sharp and unexpected macroscopic migration features, which represent an effect to be taken into account and possibly exploited to design novel scattering materials.

ACKNOWLEDGMENTS

The authors thank F. Martelli and M. Burresi for fruitful discussion. This work is financially supported by the ERC Advanced Grant PhotBots (Project No. 291349) funded under Grant No. FP7-IDEAS-ERC. C.T. and G.M. acknowledge financial support from the MIUR program Atom-Based Nanotechnology and Ente Cassa di Risparmio di Firenze through the project GRANCASSA.

[1] A. Ishimaru, *Wave Propagation and Scattering in Random Media* (Academic, New York, 1978), Vols. 1 and 2.
[2] D. Contini, F. Martelli, and G. Zaccanti, Appl. Opt. **36**, 4587 (1997).
[3] R. Pierrat, J.-J. Greffet, and R. Carminati, J. Opt. Soc. Am. A **23**, 1106 (2006).
[4] R. Elaloufi, R. Carminati, and J.-J. Greffet, J. Opt. Soc. Am. A **21**, 1430 (2004).
[5] K. M. Yoo, F. Liu, and R. R. Alfano, Phys. Rev. Lett. **64**, 2647 (1990).
[6] C. R. Doering, T. S. Ray, and M. L. Glasser, Phys. Rev. A **45**, 825 (1992).
[7] M. Boguñá, J. M. Porra, and J. Masoliver, Phys. Rev. E **59**, 6517 (1999).
[8] Z. Q. Zhang, I. P. Jones, H. P. Schriemer, J. H. Page, D. A. Weitz, and P. Sheng, Phys. Rev. E **60**, 4843 (1999).
[9] A. Duparré and S. Kassam, Appl. Opt. **32**, 5475 (1993).
[10] M. Hammer, A. Roggan, D. Schweitzer, and G. Muller, Phys. Med. Biol. **40**, 963 (1995).
[11] L. T. Perelman, V. Backman, M. Wallace, G. Zonios, R. Manoharan, A. Nusrat, S. Shields, M. Seiler, C. Lima, T. Hamano, I. Itzkan, J. Van Dam, J. M. Crawford, and M. S. Feld, Phys. Rev. Lett. **80**, 627 (1998).
[12] D. M. de Bruin, R. H. Bremmer, V. M. Kodach, R. de Kinkelder, J. van Marle, T. G. van Leeuwen, and D. J. Faber, J. Biomed. Opt. **15**, 025001 (2010).
[13] M. Leonetti and C. López, Opt. Lett. **36**, 2824 (2011).
[14] K. M. Douglass and A. Dogariu, Opt. Lett. **34**, 3379 (2009).
[15] G. Mazzamuto, L. Pattelli, C. Toninelli, and D. S. Wiersma, New J. Phys. **18**, 023036 (2016).
[16] L. Pattelli, R. Savo, M. Burresi, and D. S. Wiersma, Light: Sci. Appl. **5**, e16090 (2016).
[17] K. Yoo and R. Alfano, Opt. Lett. **15**, 320 (1990).
[18] P. A. Lemieux, M. U. Vera, and D. J. Durian, Phys. Rev. E **57**, 4498 (1998).
[19] X. Zhang and Z.-Q. Zhang, Phys. Rev. E **66**, 016612 (2002).
[20] T. Svensson, R. Savo, E. Alerstam, K. Vynck, M. Burresi, and D. S. Wiersma, Opt. Lett. **38**, 437 (2013).
[21] N. Cherroret, S. E. Skipetrov, and B. A. van Tiggelen, Phys. Rev. E **82**, 056603 (2010).
[22] A. Tosi, A. Dalla Mora, F. Zappa, A. Gulinatti, D. Contini, A. Pifferi, L. Spinelli, A. Torricelli, and R. Cubeddu, Opt. Express **19**, 10735 (2011).
[23] T. Svensson, K. Vynck, M. Grisi, R. Savo, M. Burresi, and D. S. Wiersma, Phys. Rev. E **87**, 022120 (2013).
[24] R. H. J. Kop, P. de Vries, R. Sprik, and A. Lagendijk, Phys. Rev. Lett. **79**, 4369 (1997).
[25] J. Gómez Rivas, R. Sprik, A. Lagendijk, L. D. Noordam, and C. W. Rella, Phys. Rev. E **63**, 046613 (2001).
[26] S. A. Ramakrishna and N. Kumar, Phys. Rev. E **60**, 1381 (1999).
[27] V. Gopal, S. Anantha Ramakrishna, A. Sood, and N. Kumar, Pramana **56**, 767 (2001).
[28] E. Alerstam, Phys. Rev. E **89**, 063202 (2014).
[29] P. Barthelemy, J. Bertolotti, and D. S. Wiersma, Nature (London) **453**, 495 (2008).
[30] L. Levi, Y. Krivolapov, S. Fishman, and M. Segev, Nat. Phys. **8**, 912 (2012).
[31] N. G. Chen and J. Bai, Phys. Rev. Lett. **80**, 5321 (1998).
[32] G. Popescu, C. Mujat, and A. Dogariu, Phys. Rev. E **61**, 4523 (2000).